bioRxiv preprint doi: https://doi.org/10.1101/2024.05.02.592246; this version posted May 5, 2024. The copyright holder for this preprint (which was not certified by peer review) is the author/funder, who has granted bioRxiv a license to display the preprint in perpetuity. It is made available under aCC-BY-NC-ND 4.0 International license.

Perinatal maternal undernutrition in baboons modulates hepatic mitochondrial function but not metabolites in aging offspring.

Short title: Maternal undernutrition and offspring liver function

Daniel A. Adekunbi[1], Bowen Yang[2], Hillary F. Huber[3], Angelica M. Riojas[2], Alexander J. Moody[2], Cun Li[4], Michael Olivier[5], Peter W. Nathanielsz[4], Geoffery D. Clarke[2], Laura A. Cox[5], Adam B. Salmon[1,6]

[1]Department of Molecular Medicine and Barshop Institute for Longevity and Aging Studies, The University of Texas Health Science Center at San Antonio, Texas, USA.

[2]Research Imaging Institute, Long School of Medicine, The University of Texas Health Science Center at San Antonio, Ant Texas, USA.

[3]Southwest National Primate Research Center, Texas Biomedical Research Institute, San Antonio, Texas, USA.

[4]Texas Pregnancy and Life-course Health Research Center, Department of Animal Science, University of Wyoming, Laramie, Wyoming, USA.

[5]Center for Precision Medicine, Department of Internal Medicine, Wake Forest University School of Medicine, Winston-Salem, North Carolina, USA.

[6]Geriatric Research Education and Clinical Center, Audie L. Murphy Hospital, Southwest Veterans Health Care System, San Antonio, Texas, USA.

Corresponding author: Dr. Adam Salmon, Barshop Institute for Longevity and Aging Studies, The University of Texas Health Science Center at San Antonio, 7703 Floyd Curl Dr, San Antonio TX, 78229. Texas, USA (email: salmona@uthscsa.edu)

bioRxiv preprint doi: https://doi.org/10.1101/2024.05.02.592246; this version posted May 5, 2024. The copyright holder for this preprint (which was not certified by peer review) is the author/funder, who has granted bioRxiv a license to display the preprint in perpetuity. It is made available under aCC-BY-NC-ND 4.0 International license.

Abstract

We previously demonstrated in baboons that maternal undernutrition (MUN), achieved by 70 % of control nutrition, impairs fetal liver function, but long-term changes associated with aging in this model remain unexplored. Here, we assessed clinical phenotypes of liver function, mitochondrial bioenergetics, and protein abundance in adult male and female baboons exposed to MUN during pregnancy and lactation and their control counterparts. Plasma liver enzymes were assessed enzymatically. Liver glycogen, choline, and lipid concentrations were quantified by magnetic resonance spectroscopy. Mitochondrial respiration in primary hepatocytes under standard culture conditions and in response to metabolic (1 mM glucose) and oxidative (100 µM H_2O_2) stress were assessed with Seahorse XFe96. Hepatocyte mitochondrial membrane potential (MMP) and protein abundance were determined by tetramethylrhodamine ethyl ester staining and immunoblotting, respectively. Liver enzymes and metabolite concentrations were largely unaffected by MUN, except for higher aspartate aminotransferase levels in MUN offspring when male and female data were combined. Oxygen consumption rate, extracellular acidification rate, and MMP were significantly higher in male MUN offspring relative to control animals under standard culture. However, in females, cellular respiration was similar in control and MUN offspring. In response to low glucose challenge, only control male hepatocytes were resistant to low glucose-stimulated increase in basal and ATP-linked respiration. H_2O_2 did not affect hepatocyte mitochondrial respiration. Protein markers of mitochondrial respiratory chain subunits, biogenesis, dynamics, and antioxidant enzymes were unchanged. Male-specific increases in mitochondrial bioenergetics in MUN offspring may be associated with increased energy demand in these animals. The similarity in systemic liver parameters suggests that changes in hepatocyte bioenergetics capacity precede detectable circulatory hepatic defects in MUN offspring and that the mitochondria may be an orchestrator of liver programming outcome.

Keywords: developmental programming; baboons; liver; bioenergetics; hepatocytes

bioRxiv preprint doi: https://doi.org/10.1101/2024.05.02.592246; this version posted May 5, 2024. The copyright holder for this preprint (which was not certified by peer review) is the author/funder, who has granted bioRxiv a license to display the preprint in perpetuity. It is made available under aCC-BY-NC-ND 4.0 International license.

1.0. Introduction

Suboptimal nutrition during the developmental period, from *in utero* through early life development, is common among individuals from disadvantaged populations. Nutritional perturbations during these critical periods can induce long-standing physiological changes that increase risk of developing chronic diseases, including metabolic diseases, later in life. In response to nutritional stress during pregnancy, the fetus initiates adaptive processes to ensure its survival albeit at the expense of optimal structural and functional development. The mechanisms by which early-life exposures and challenges increase susceptibility to adult-onset diseases are not entirely clear, but it is likely that adaptive process to ensure fetal survival likely come at the expense of optimal structural and functional development that persist throughout life[1,2].

The liver has been shown to be keenly sensitive to *in utero* nutrient restriction[3], and fetal liver size is reduced under this challenge in various species including rats, sheep, cattle, baboons, and humans among others[4-8]. We and others have also reported alterations in fetal liver metabolites and gene expression patterns due to maternal nutrient reduction[6,9-11]. Although several other animal models have shown association between maternal undernutrition (MUN) and disrupted metabolism in adulthood[12,13], there is a need to study nonhuman primates due to their close phylogenetic relationship and similar physiology to humans[14] to bridge the translational gap in developmental programming studies. We previously noted the emergence of insulin resistance in juvenile (3.5 years) offspring of baboons exposed to moderate MUN during pregnancy and lactation[15]. The liver undergoes several functional changes during the early postnatal period before achieving full maturation[16] and developmental programming imprints persist throughout development and early adulthood of the offspring. Long-term changes associated with aging in this model remain unexplored.

Metabolic disorders are primarily driven by disruption in energy homeostasis, of which the mitochondria can play a key role. Mitochondria play multitude of roles in regulating energy balance including ATP production, generation of reactive oxygen species (ROS) and regulating cellular signaling pathways, and impairment of these systems contribute to metabolic dysfunction. Developmental programming of critical component systems such as the mitochondria has been proposed as a cellular mechanism by which maternal effects are propagated in the offspring given the developmental plasticity of the mitochondria and maternal imprints in the offspring mitochondrial genome[17]. Our recent study demonstrated that MUN impaired fetal mitochondrial structure and function, including alterations in mitochondrial cristae and bioenergetics in cardiac tissue[18]. Impairment in fetal mitochondrial function is linked to compromised metabolic health in postnatal life[19], and cumulative damage to the mitochondria is suggested to trigger the onset of many age-related diseases[20]. In line with this, we have shown that MUN in baboons drives mitochondrial bioenergetic defects that persist even to adulthood in skin-derived fibroblasts[21].

As a follow-up to our previous studies[10,11,13], we utilized baboons with an average age of 15 years (approximate human equivalent; 60 years), representing animals in or transitioning to the late stage of life, to investigate the long-term impact of MUN on the liver at the functional and molecular level. In the present study, we assessed clinical phenotypes of liver function by analyzing plasma changes in liver enzymes to identify functional hepatic deficits related to MUN in the aging offspring. Additionally, we examined lipid accumulation and other metabolites in the liver using magnetic resonance spectroscopy. Considering the possibility that subcellular changes may present

bioRxiv preprint doi: https://doi.org/10.1101/2024.05.02.592246; this version posted May 5, 2024. The copyright holder for this preprint (which was not certified by peer review) is the author/funder, who has granted bioRxiv a license to display the preprint in perpetuity. It is made available under aCC-BY-NC-ND 4.0 International license.

earlier than phenotypic alterations, that is, systemic outcomes are preceded by cellular changes, we assessed mitochondrial bioenergetics and cellular protein abundance in primary hepatocytes derived from these animals.

2.0. Methods

2.1. Animals

The Institutional Animal Care and Use Committee of Texas Biomedical Research Institute (TBRI) approved all procedures involving animals. The animal facilities at the Southwest National Primate Research Center (SNPRC), housed on TBRI campus are fully accredited by the Association for Assessment and Accreditation of Laboratory Animal Care International (AAALAC), and adheres to the guidelines of the National Institutes of Health (NIH) and the U.S. Department of Agriculture.

Details of animal husbandry and establishment of MNR model have been published previously by our group[22, 23]. Baboons (*Papio* sp.) were housed and maintained in a social environment and fed ad libitum with normal monkey diet. The welfare of the animals was enhanced by providing enrichments, such as toys, food treats, and music, which were offered daily under the supervision of the veterinary and behavioral staff at SNPRC.

The baboon colony used in this study were established more than 20 years ago. To develop the MUN cohort, age-matched females were randomly assigned prior to breeding to control or MUN group. Control mothers had *ad libitum* access to water and SNPRC biscuits (Purina Monkey Diet and Monkey Diet Jumbo, Purina LabDiets, St Louis, MO, USA) containing 12% energy from fat, 0.29% from glucose, 0.32% from fructose, and a metabolizable energy content of 3.07 kcal/g. MUN group were fed 70% of the feed eaten by the control females on a weight-adjusted basis from the time of diagnosis of pregnancy (~30 days gestation) for the rest of pregnancy and through lactation. We have previously demonstrated that MUN leads to intrauterine growth restriction (IUGR) at term[24]. Both control and MUN offspring were weaned at 9 months and maintained on Purina Monkey diet through adulthood. Animals were euthanized at ages ranging between 13 and 18 years (approximate human equivalent, 50 and 70 years).

2.2. Magnetic resonance spectroscopy

All proton magnetic resonance spectroscopy (1H-MRS) experiments were conducted on a Siemens 3T system (Trio, Siemens Healthcare, Malvern, PA) with a transmitting body coil. The scans were carried out when the animals were approximately 14 years old. We used straps to minimize involuntary motion during the scanning protocols. MRI scans were performed while subjects were mechanically ventilated and under sedation according to the following protocol: After an overnight fast (12 h), each baboon was sedated with ketamine hydrochloride (10 mg/kg i.m.) before arrival at the MRI room. Endotracheal intubation was performed using disposable cuffed tubes (6.5 - 8.0 mm diameter) under direct laryngoscopic visualization. All animals were supported with 98 - 99.5% fraction of inspired oxygen (FiO_2) by a pressure-controlled ventilator adjusted, as necessary, to keep the oxygen saturation >95%. The maintenance of anesthesia consisted of an inhaled isofluorane (0.5 - 1.5%) and oxygen mix.

Glycogen, choline, and lipid concentrations in the liver were quantified using single-voxel, spin echo localized 1H-MRS[25]. A voxel with a volume of 12x12x12 mm^3 was placed in the right posterior love of the liver. The voxel was placed approximately 2 cm within Gleason's capsule to avoid signal contamination from the visceral adipose compartment. Due to the amplitude of the water resonance, two spectra were collected for each subject: a water

bioRxiv preprint doi: https://doi.org/10.1101/2024.05.02.592246; this version posted May 5, 2024. The copyright holder for this preprint (which was not certified by peer review) is the author/funder, who has granted bioRxiv a license to display the preprint in perpetuity. It is made available under aCC-BY-NC-ND 4.0 International license.

reference (TR = 2000 ms, TE = 30 ms, NSA = 8) and a water-saturated spectrum (TR = 2000 ms, TE = 30 ms, NSA = 16).

2.3. 1H-MRS data processing

All spectral peaks were fit using the non-linear least squares, an advanced method for the accurate, robust, and efficient spectral fitting algorithm (AMARES) in the Java-based magnetic resonance user interface software (jMRUI v5.2). The detailed process of analyzing 1H-MRS data has been previously described[25, 26]. Firstly, to reduce fitting residuals, MRS data are processed by fitting spectral peaks using the spectral-fitting algorithm in the MRS analysis software jMRUI. Spectra were corrected for phase offsets by applying a phase shift not exceeding ± 12 for either the reference or unsuppressed spectra. Secondly, if any residual water resonance was present for water-suppressed spectra, it was removed by applying the Hankel Lanczos singular value decomposition (HL-SVD) filter with no point maxima. The reference peak was assigned to the water peak (in unsuppressed spectra). Water-suppressed spectra were also filtered using apodization with a 3.5 Hz Gaussian. Water signals are generated from the water-unpressed spectrum. During the jMRUI analysis, starting values and prior knowledge estimates were applied according to previous publications[25, 27, 28]. Since there is an inherent signal loss at the point of data acquisition, glycogen, choline, and lipid signals were corrected by T2 relaxation[25, 27].

2.4. Tissue Collection

At approximately 15 years of age, male and female adult baboons were tranquilized with ketamine hydrochloride (10 mg/kg i.m.) after an overnight fast. Three days prior to necropsy, morphometrics including body weight and length were determined to calculate body mass index and blood samples drawn through the femoral vein to obtain plasma for liver enzymes analyses. On the day of necropsy, tranquilized baboons were exsanguinated while still under general anesthesia as approved by the American Veterinary Medical Association. Following failure of reflex responses to skin pinch and eye touch stimulation, liver tissues were rapidly removed and weighed. Tissues were collected between 8.00-10.00 AM to minimize potential variation from circadian rhythm. Left and right liver lobes were separated apart, about 30 grams of each lobe was cut laterally closer to the caudal portion of the liver and received into an ice-chilled 1X HBBS for subsequent hepatocyte isolation. The remaining liver portion was immediately frozen in liquid nitrogen for other analyses as part of other investigations. All necropsies were performed by qualified and experienced veterinarians.

2.5. Plasma liver enzyme quantification

Markers of liver function including aspartate aminotransferase (AST), alkaline phosphatase (ALP), and alanine aminotransferase (ALT) were assessed in plasma samples using the Beckman Coulter UniCel DxC 800 Synchron Clinical System (Brea, CA, USA) along with their specific reagents from Beckman Coulter. AST, ALP, and ALT were measured using enzymatic rate method[29].

2.6. Hepatocyte cultures

The two-step EGTA/collagenase perfusion technique[30, 31] was adapted to isolate primary hepatocytes from baboon liver ex situ. Liver samples were processed within 1 h post collection to achieve viable hepatocytes. Two cannulae (16g x 4in) with a 3 mm smooth olive-shaped tip were positioned to target vascular channels in the liver for perfusion. The liver was first perfused an EGTA solution that comprised 0.14M NaCl, 50 mM KCL, 0.33 mM

bioRxiv preprint doi: https://doi.org/10.1101/2024.05.02.592246; this version posted May 5, 2024. The copyright holder for this preprint (which was not certified by peer review) is the author/funder, who has granted bioRxiv a license to display the preprint in perpetuity. It is made available under aCC-BY-NC-ND 4.0 International license.

Na_2HPO4, 0.44 mM KH_2PO4, 10 mM Na-HEPES, 0.5 mM EGTA, 5 mM Glucose, and 4 mM $NaHCO_3$ with pH adjusted to 7.2 using a Masterflex peristaltic pump (Cole-Palmer, Niles, IL, USA) set at a rate of 10 revolutions per minute (rpm), for approximately 1 h at 37 °C[32].

Following perfusion with the EGTA buffer, the solution was replaced with a collagenase solution which comprises 0.1 % collagenase, 5 mM $CaCl_2$, and 4 mM $NaHCO_3$ in 1X HBSS solution (0.14 M NaCl, 50 mM KCL, 0.33 mM Na_2HPO4, 0.44 mM KH_2PO4, 10 mM Na-HEPES), pH 7.5. The perfusion was maintained at a rate of 8 rpm for approximately 1 h or until visible sign of digestion identified by liver indentation following gentle pressure or obvious cell dissociation through the Glisson's capsule that overlays the liver. The digested liver is collected into a tissue culture dish containing chilled Gibco's Williams media that is supplemented with 5% FBS, 1% glutamine, and antibiotics. Cell suspensions were filtered through sterile folded gauze, centrifuged at 50 g, 4°C for 5 min. The centrifugation step was repeated twice, and the resulting hepatocytes were assessed for viability using trypan blue dye. Cultures plates were coated with collagen (Collagen, Type 1 from rat tail, Sigma, Saint Louis, MO) diluted 1 to 50 ratio in sterile H_2O prior to cell seeding. Hepatocytes were allowed to adhere overnight before further experiments.

2.7. Seahorse mitochondrial assay

To assess cellular respiration in primary baboon hepatocytes from control and MUN baboons, we used Agilent Seahorse XF96 Extracellular Flux Analyzer (North Billerica, MA, USA). Hepatocytes were plated in a collagen-coated 96-well seahorse plate at a density of 40,000 cells per well. The XFe96 sensor cartridges were hydrated overnight with H_2O at 37 °C and replaced with seahorse XF calibrant 1 h before the assay. Oxygen consumption rate (OCR) and extracellular acidification rate (ECAR) were measured under basal condition and in response to serial injection of mitochondrial inhibitors including 1.5µM Oligomycin (to inhibit ATP synthase), 0.5 µM FCCP (Carbonyl cyanide-p-trifluoromethoxyphenylhydrazone; a mitochondrial uncoupler to measure maximum respiration) and 0.5 µM antimycin A and rotenone cocktail (to inhibit electron flow through the mitochondrial electron transport chain). We also determined OCR in response to 2 h exposure to 1 mM glucose or 100 µM H_2O_2 to model metabolic and oxidative stress respectively prior to the seahorse assay. OCR were normalized to cell density per well measured by a live-cell imaging system (IncuCyte S3, Santorius Corporation, Edgewood, NY, USA). Data were processed using the Agilent wave software.

2.8. Hepatocyte mitochondrial membrane potential.

Mitochondrial membrane potential was determined using tetramethylrhodamine ethyl ester (TMRE) kit from Abcam. TMRE is a cell-permeant dye that accumulates in active mitochondria due to their relative negative charge. Hepatocytes (5,000 cells) were seeded in black-walled 96-well plates and incubated with media containing 200 nM TMRE for 20 min at 37 ^{o}C. Following incubation, cells were washed with phosphate-buffered saline, and fluorescence intensity captured using the IncuCyte (Red excitation: 567-607 nM and emission: 622-704 nM). FCCP (20 µM) was used as internal control as it prevents TMRE staining, and its signal was used to set the minimum intensity threshold for TMRE during data analysis. TMRE fluorescence intensity per image was normalized to phase image area.

2.9. Hepatocyte protein expression by immunoblotting

bioRxiv preprint doi: https://doi.org/10.1101/2024.05.02.592246; this version posted May 5, 2024. The copyright holder for this preprint (which was not certified by peer review) is the author/funder, who has granted bioRxiv a license to display the preprint in perpetuity. It is made available under aCC-BY-NC-ND 4.0 International license.

Cell homogenates for immunoblotting were prepared using commercially available RIPA buffer (Thermo Scientific, Waltham, MA, USA). The concentration of protein in the homogenates was determined by colorimetric protein assay[33]. Equal amounts of protein extract (15 µg) were separated by SDS- polyacrylamide gel electrophoresis (5 % staking and 12 % resolving gel) and transferred to a nitrocellulose membrane. Antibodies for individual components of the mitochondrial electron transport chain (ETC) complexes I-V (NDFUB8, SDHB, UQCRC2, MTCO1 and ATP5α), mitofusin 1 (MFN 1), dynamin-related protein 1 (Drp1), optic atrophy protein 1 (OPA1), peroxisome proliferator-activated receptor-gamma coactivator 1-alpha (PGC1a), catalase and superoxide dismutase 2 (SOD2), were incubated overnight in 2% BSA at 4^{o}C. ETC complexes antibodies were assayed together as part of total OXPHOS antibody cocktail. Other primary antibody details are provided in table 1. Protein bands for each sample were visualized using LI-COR imaging system after 1 h incubation with LI-COR IRDye® 800CW goat anti-mouse and anti-rabbit secondary antibodies (LI-COR Biosciences, Lincoln, NE, USA). All immunoblots were quantified using LI-COR Image Studio Lite software.

Table 1: Primary antibodies for immunoblotting

Antibody	**Dilution ratio**	**Company**	**Cat #**
Total OXPHOS	1:2,000	Abcam	ab110411
MFN1	1:1,000	Abcam	ab221661
Drp1	1:1,000	Cell Signaling	8570
OPA1	1:1,000	Cell Signaling	80471
PGC1a	1:500	Cell Signaling	2173
Catalase	1:1,000	Cell Signaling	14097
SOD2	1:1,000	Abcam	ab13533
Vinculin	1: 10,000	Cell Signaling	4650

2.9. Statistical analysis

Data were analyzed by two-way analysis of variance (ANOVA) followed by Tukey post hoc test for multiple comparison and unpaired t-test when comparing effects between two groups. The ANOVA was weighted using SEM to account for variability in technical replicates. We did not observe any significant variation in hepatocyte data generated from the left and right liver lobe and were therefore pooled for subsequent analyses. Control male and female baboons were aged between 13.6-18.0 and 13.3-16.5 years, respectively, while MUN baboons were aged 13.7–16.2 years for males and 13.3-16.5 years for females. Data are presented as mean □±□ SEM; $p<0.05$ is considered statistically significant. All analyses were carried out using GraphPad prism 9.

3.0. Results

3.1. Liver metabolites

bioRxiv preprint doi: https://doi.org/10.1101/2024.05.02.592246; this version posted May 5, 2024. The copyright holder for this preprint (which was not certified by peer review) is the author/funder, who has granted bioRxiv a license to display the preprint in perpetuity. It is made available under aCC-BY-NC-ND 4.0 International license.

The concentrations of glycogen, choline and lipid in the liver measured by 1H-MRS were similar in both male and female MUN offspring when compared to their control counterparts. When male and female data were combined, the levels of these liver metabolites remained comparable between control and MUN baboons. Liver lipid concentration tended to be higher in control (p=0.095) relative to MUN baboons though these did not reach statistical significance (Fig. 1).

3.2. Anthropometric variables and relative liver weight

Animals used in this study were aged-matched and there was no effect of MUN on body weight or body mass index (BMI) at this stage in later life. Overall, male baboon body weight was significantly higher than female in both control and MUN offspring. This sex-related difference in body weight is a well-recognized physiological factor. The relative liver weight, determined by the ratio of liver weight to body weight was similar between MUN and control offspring (Table 2).

Table 2: Anthropometric measures and relative liver weight in adult control and MUN baboons

Group	**CTR**		**MUN**		**ANOVA**
	M	F	M	F	
Subject total	7	10	6	7	
Age (year)	16.4 ± 0.6	15.6 ± 0.5	15.1 ± 0.5	14.2 ± 0.5	NS
Weight (kg)	26.7 ± 1.6	18.6 ± 1.3	30.8 ± 1.3	18.8 ± 1.2	M > F *
BMI (kg/m^2)	17.9 ± 0.8	15.8 ± 0.7	20.3 ± 1.0	17.0 ± 1.2	NS
Relative liver weight (%)	1.60 ± 0.07	1.59 ± 0.07	1.39 ± 0.10	1.66 ± 0.26	NS

*p < 0.05; NS, not significant. Abbreviations: CTR; control offspring, MUN; maternal undernutrition offspring

3.3. Liver enzymes

We compared plasma concentrations of AST, ALP, and ALT between control and MUN offspring as markers of liver function to determine the long-term impact of developmental undernutrition in adulthood. There were no significant differences in plasma liver enzyme levels between the groups when analyzed by sex independently. However, combined male and female data of control and MUN offspring showed significantly higher AST concentrations in MUN compared to control while ALP and ALT concentrations remained similar (Fig. 2).

3.4. Hepatocyte number and viability.

We next asked whether MUN had affects in adults at the hepatic cellular level using isolated hepatocytes from these animals to determine if MUN induce changes in cell physiology using readouts of cell viability and mitochondrial function (discussed below). Figure 3 shows that the number of live hepatocytes per gram of liver tissue as well as hepatocyte viability were similar between control and MUN baboons.

3.5. Hepatocyte bioenergetics

bioRxiv preprint doi: https://doi.org/10.1101/2024.05.02.592246; this version posted May 5, 2024. The copyright holder for this preprint (which was not certified by peer review) is the author/funder, who has granted bioRxiv a license to display the preprint in perpetuity. It is made available under aCC-BY-NC-ND 4.0 International license.

We assessed hepatocyte bioenergetics using a mitochondrial stress test and show that OCR and ECAR were significantly higher in female-derived hepatocytes compared to males in control offspring. However, in MUN offspring there were no sex-differences in OCR and ECAR between male and female suggesting perhaps that early-life nutrient reduction may affect hepatic respiration sexual dimorphism. OCR parameters including basal respiration, ATP-linked respiration, maximal respiration, and spare respiratory capacity and ECAR were similar between in control and MUN female offspring. However, in male offspring, these parameters were significantly higher in hepatocytes from MUN offspring compared to hepatocytes from control animals (Fig. 4 a-d). Thus, MUN appears to have a male-specific effect on hepatic mitochondrial bioenergetics. The ratio of OCR to ECAR was also similar between the experimental groups (Fig. 4 e and f) suggesting no dramatic changes in mitochondrial fuel preference.

Mitochondrial membrane potential (MMP) was also significantly affected by MUN in isolated hepatocytes. Samples from MUN female offspring exhibit lower MMP when compared to their control counterparts, whereas in males, MMP was higher in MUN animals compared to controls. The MMP data correspond somewhat to the differences observed in OCR between MUN and control baboons, particularly in males. Additionally, we noted higher MMP in control females relative to males whereas the opposite was observed in MUN animals (Fig. 4 g).

3.6. Hepatocyte bioenergetics in response to low glucose and H_2O_2

We next asked whether MUN affected the response of hepatocytes from adult offspring to metabolic challenge in culture. In female-derived samples, hepatocytes exposed to low glucose (1mM) exhibited a significantly increased basal and ATP-linked respiration relative to standard glucose conditions in both control and MUN. However, maximum respiration and energy reserve were reduced in response to low glucose. These changes were observed in both control and MUN offspring suggesting MUN did not affect hepatocyte response to metabolic challenge in females (Fig. 5 a-d).

Unlike in females, male-derived hepatocytes showed low glucose-stimulated increase in basal and ATP-linked respiration only in MUN offspring. One interpretation is that increased OCR in MUN baboons might represent an increased energy demand in these cells under challenge. Hepatocytes from male MUN offspring also showed reduced maximal respiration following low glucose exposure. Low glucose challenge also ablated the difference in spare respiratory capacity we report between MUN and control hepatocytes under standard culture conditions (Fig. 5 e-f).

We also asked whether exposing hepatocytes to H_2O_2 (an inducer of oxidative stress) would reveal differences in bioenergetic response between control and MUN. However, this challenge did not significantly affect hepatocyte respiration except for a reduction in basal respiration in female MUN group following exposure to H_2O_2 (Supplemental Fig. 1). Furthermore, low glucose or 100 µM H_2O_2 elicited nearly identical changes in mitochondrial membrane potential similar to untreated cells in control and MUN baboons of both sexes (Supplemental Fig. 2).

3.7. Protein expression

We asked if the differences in bioenergetics in hepatocytes might be explained by mitochondrial content differences. The levels of OXPHOS proteins; complex I (NDUFB8), complex II (SDHB), complex III (UQCRC2), complex IV (MTCO1), and complex V (ATP5α) in isolated hepatocytes were not different between control and

bioRxiv preprint doi: https://doi.org/10.1101/2024.05.02.592246; this version posted May 5, 2024. The copyright holder for this preprint (which was not certified by peer review) is the author/funder, who has granted bioRxiv a license to display the preprint in perpetuity. It is made available under aCC-BY-NC-ND 4.0 International license.

MUN offspring of both sexes (Fig. 7). This suggests the differences in bioenergetics we report is likely not related to mitochondrial abundance in these cell lines. Consistent with mitochondrial content, mitochondrial fusion proteins (MFN1 and OPA1) and fission protein (Drp1) were similar between the groups (Fig. 8 a-e). The marker of mitochondrial biogenesis (PGC1a) was also unchanged (Fig 8. f and h). The protein levels of antioxidant enzymes; catalase and SOD2 were not also altered in both male and female MUN baboons relative to their aged-matched controls.

4.0. Discussion

Our study shows that developmental programming imprints in baboons are notably evident at the cellular level, even in late adulthood, with primary hepatocytes derived from male MUN offspring highly sensitive to modulators of the mitochondrial electron transport chain, resulting in elevated OCR parameters relative to control offspring but without major changes to systemic liver function. The observed sexual dimorphism in mitochondrial OCR is consistent with the predominantly male-centric effect of programming in several metabolic studies. We previously reported male specific effects of MUN on genes regulating hepatic energy metabolism in fetal baboon liver and adipose tissue[34]. Postnatally, MUN also induces pericardial adiposity in 6-year-old male offspring but not in females[34]. Increased serum level of total cholesterol and low-density lipoprotein were also observed only in male MUN offspring at 9 years of age[35]. This study adds to the male-specific effects of MUN on mitochondrial bioenergetic parameters in hepatocytes derived from the aging offspring. Baboon lifespan has been reported as 11 or 21 years[36,37] and thus, the animals used in this study aged between 13 and 18 years represent the transition period from mid- to late-life. Another interesting finding from this study is that mitochondrial OCR parameters are higher in female derived hepatocytes compared to male in control baboons, which agrees with other studies using liver tissue in mice[38]. It is not clear if this observation relates to estrogen signaling and translates to any protective effect in the female, in line with estrogen protective role against hepatic steatosis[39]. In male and female MUN offspring, we did not observe any sex differences, suggesting MUN abrogated this sexual dimorphism in mitochondrial respiration.

While most liver metabolic markers we examined were unaffected by MUN at the time of sampling, the changes in hepatocyte mitochondrial respiration may indicate a tendency for metabolic alterations particularly in the male animals. We view the similarity in liver metabolic phenotypes between MUN and control offspring as adaptive which could be altered in the presence of a second physiological insult overlaid on the perinatal exposure in adulthood. An adaptive response to poor perinatal nutrition triggers susceptibility to metabolic diseases in adulthood especially following exposures to nutritional challenge later in life. For example, postnatal catch-up growth following IUGR leads to obesity especially when the offspring are fed a hypercaloric diet[40]. Our study model did not incorporate any secondary challenge following the perinatal nutrient reduction but focused on the long-term perpetuation of programming effect, thus outcomes are representative of basal effects. However, our low glucose metabolic challenge results in hepatocytes are consistent with this idea.

We previously reported that MUN leads to reduced fetal liver weight, changes in fetal liver metabolites, smaller body weight at birth, juvenile prediabetic phenotype and altered lipid metabolism in young adulthood [7,10,11,15,35]. There are few studies on the long-term impact of MUN on liver function in precocial species and to our knowledge,

bioRxiv preprint doi: https://doi.org/10.1101/2024.05.02.592246; this version posted May 5, 2024. The copyright holder for this preprint (which was not certified by peer review) is the author/funder, who has granted bioRxiv a license to display the preprint in perpetuity. It is made available under aCC-BY-NC-ND 4.0 International license.

none specifically in aging NHP such as baboons, which share 96% genetic homology with humans[41]. Our study model could therefore address many confounding factors in human studies that limit clear delineation of the impact of MUN on liver function separate from secondary metabolic challenges like obesogenic feeding in adulthood. For example, in a Chinese famine cohort study, fetal and infant exposure to famine was linked to an increased risk of fatty liver disease in female offspring five decades later. However, these subjects were also obese, and the contribution of obesity in adulthood was not factored into the analyses[42]. Similarly, participants from the Helsinki Birth Cohort who were smaller during early childhood exhibited an elevated risk of fatty liver disease in adulthood but as obese subjects[43]. Thus, the relationship between early-life malnutrition and risk of hepatic disease, independent of adult overweight/obesity, remains unclear. In the present study, MUN offspring maintained similar body weight as control offspring, despite early postnatal catch-up growth[23] and we did not see any clinical features of hepatic dysfunction in the MUN offspring; liver weight, hepatic glycogen, choline, and lipid content were similar to control offspring. Plasma markers of liver function were also unchanged except for higher AST levels in MUN offspring when male and female data were combined. Our results suggest that independent of an additional metabolic insult in adulthood, there are no signs of liver disease in aging MUN baboon offspring, despite potential cellular metabolic differences.

In a previous study by our group on the effects of MUN on liver function in aging sheep[44], we observed that a 50 % nutrient restriction during early pregnancy did not alter liver weight in the female offspring at 6 years of age, average lifespan of a sheep is 7 years[45], while liver glycogen content only tended to be greater in the MUN offspring compared to control. Meanwhile, the MUN offspring had elevated hepatic lipid levels and low expression of peroxisome proliferator-activated receptor-γ (PPARγ), a transcriptional regulator that modulates fat metabolism. Additionally, they had higher body weight compared to the control group[44], suggesting a potential link between disturbance to liver metabolic function in MUN offspring and the occurrence of obesity. A different group demonstrated that MUN during early pregnancy in sheep resulted in small liver size in middle-aged male offspring, independent of changes to total body mass[12]. The changes in liver mass parallel a significant reduction in hepatocyte growth factor genes in the liver of the same animals. Even in the same species, there are variability in programming outcome on liver function likely due to the type of nutritional constraint, sex, body weight status and age at examination.

Early studies have demonstrated the hepatic mitochondrial dysfunction precedes the development of non-alcoholic fatty liver diseases[46]. Thus, animals can present normal circulatory metabolic phenotype concurrently with altered hepatic mitochondrial structure and function. We view the mitochondria as an early target organelle of developmental programming because the broad range of phenotypes of adverse perinatal exposures suggest the involvement of a common or integrative mechanism across different cells and tissues than individual molecular markers. Mitochondrial vulnerability to damage begins early. Mitochondria of fertilized oocytes are susceptible to damage from poor gestational conditions, these mitochondrial defects persist into fetal and postnatal life and are linked to increased risk of diseases including metabolic disorders[19,47-49]. We previously demonstrated that MUN during pregnancy increases activity of the fetal hypothalamic-pituitary-adrenal axis, evidenced by high cortisol and ACTH concentrations in near-term baboons[50]. Further, we have observed a rise in local cortisol production in male fetal liver under MUN conditions[34]. This hormonal milieu may contribute to programmed changes in liver mitochondria, potentially influencing hepatocyte bioenergetic capacity in adulthood, as demonstrated in this study.

bioRxiv preprint doi: https://doi.org/10.1101/2024.05.02.592246; this version posted May 5, 2024. The copyright holder for this preprint (which was not certified by peer review) is the author/funder, who has granted bioRxiv a license to display the preprint in perpetuity. It is made available under aCC-BY-NC-ND 4.0 International license.

Mitochondria participate in stress responses, with glucocorticoid receptors also expressed within the mitochondria[51]. In response to stress, cells consume more energy to maintain their viability, either for the synthesis of biomolecules required for growth or protective efficiency such as repair of cellular damage and return to homeostasis[52,53]. The higher OCR parameters in hepatocytes derived from male MUN offspring under standard cell culture conditions may reflect an adaptive response from perinatal nutritional exposure resulting in elevated energy demand to meet cellular processes such as gene transcription and translation which may be at a higher metabolic cost due to programming.

Alternatively, the higher OCR in male MUN hepatocytes may indicate a state of programmed hypermetabolism, that is, increased resting energy expenditure[51] to maintain normal liver function following perinatal challenge. This energy budget may drive the similarity we observed in liver metabolites and markers of liver function at the systemic level between control and MUN offspring, albeit at a high energetic cost. The increased OCR is consistent with and corresponds to higher MMP; measured by accumulation of fluorescent cation TMRE within the mitochondrial matrix. The magnitude of MMP increase in male MUN offspring relative to control offspring suggests mitochondrial hyperpolarization likely due to hyperactivity of the proton pump in the mitochondrial respiratory chain. Mitochondrial hyperpolarization is associated with excessive ROS production which eventually triggers cell death[54]. It is important to note that changes in cell volume may influence TMRE fluorescence intensity. Since we normalized signals with cell area, changes in cell structure are unlikely to influence TMRE signals in our study. A sustained hypermetabolic state along with increased ROS production may eventually overwhelm defense capability of the antioxidant system, indicating potential for increased vulnerability to 'wear-and-tear' in the male MUN offspring. Moreso, stress-induced hypermetabolism has been reported to accelerate rates of aging[55]. Although, we did not measure ROS activity in the hepatocytes, the similar level of antioxidant proteins in both control and MUN offspring suggest the buffering capacity against oxidative stress may be lower in male MUN offspring. A related study also demonstrated that prenatal exposure to maternal stress is associated with higher leukocyte mitochondrial content and bioenergetic capacity in the offspring[56], highlighting the potential significance of bioenergetic capacity among other mitochondrial phenotypes (e.g. mitochondrial biogenesis) in developmental programming. The similarity in protein markers of ETC subunits (complex I-V), mitochondrial biogenesis (PGC1a) and mitochondrial dynamics (MFN1, OPA1, and Drp1) between the experimental groups suggests that mitochondrial protein content or remodeling of mitochondrial network through fusion and fission processes does not contribute to the increased bioenergetic capacity of the male MUN offspring.

Similar to other reports showing increased cellular OCR in response to acute low glucose exposure[57], basal and ATP-linked respiration in male MUN hepatocytes were further elevated by low glucose exposure, while control males were unaffected, which may indicate adaptation to metabolic challenge in control males. We can as well speculate that the high basal and ATP-linked OCR mimics a stress response to meet increased energy demand. It could also be related to oxidation of other fuel substrates like lipids in the absence of glucose, to sustain cell viability. The latter is more plausible since it has been demonstrated that low glucose increases dependency on fatty acid oxidation for basal mitochondrial metabolism[58]. Comparing this low glucose-stimulated increase in OCR parameters with the higher OCR in MUN male hepatocytes cultured in standard glucose media, fits the narrative that a similar mechanism that enhances basal respiration under low glucose raises hepatocyte respiration of male MUN offspring under standard culture conditions and thus represent stress responses. In females, low-glucose

bioRxiv preprint doi: https://doi.org/10.1101/2024.05.02.592246; this version posted May 5, 2024. The copyright holder for this preprint (which was not certified by peer review) is the author/funder, who has granted bioRxiv a license to display the preprint in perpetuity. It is made available under aCC-BY-NC-ND 4.0 International license.

stimulated increase in basal and ATP-linked OCR were similar in control and MUN offspring, corroborating the perpetuation of male-specific effects in response to metabolic challenge. However, despite the stimulation of basal OCR by low glucose, energy reserve was drastically reduced following the metabolic stress, suggesting low glucose limits achievable maximal respiration. This reduction in energy reserve following exposure to low glucose is consistent with other studies[59]. In relation to oxidative stress challenge, we did not find major changes to the pattern of cellular respiration between the groups when hepatocytes were exposed to H_2O_2, which may relate to the concentration of H_2O_2 we tested.

In our baboon MUN model, aging male MUN offspring exhibit changes in mitochondrial bioenergetic parameters without concurrent systemic liver function alterations. This supports the idea that hepatic mitochondrial dysfunction may precede detectable circulatory defects[46]. There is a potential to detect hepatic defects if our study had more sample size as the combination of male and female data showed a significant increase in AST level in MUN offspring. Overall, this study suggests that changes to mitochondrial function may be an orchestrator of programming effect on liver function in adulthood.

Acknowledgements

The authors express their gratitude to the Research Imaging Institute and the Southwest National Primate Center Staff for their continuous technical support in our baboon research program. We also acknowledge the administrative and technical support of Karen Moore, Wenbo Qi, Benjamin Morr, Kevin Thyne, Jonathan Gelfond, and Raechel Camones.

Financial Support

This work was supported by the National Institute on Aging (ABS; AG057431, PWN and LAC; 1U19AG057758), the San Antonio Nathan Shock Center (P30 AG 013319). The baboon facility at the SNPRC is supported by National Institutes of Health (P51 OD011133). This material is the result of work supported with resources and the use of facilities at South Texas Veterans Health Care System, San Antonio, Texas. The contents do not represent the views of the U.S. Department of Veterans Affairs or the US Government.

Competing Interest

The authors declare no competing interest.

Reference

1. Wu G, Bazer FW, Cudd TA, Meininger CJ, Spencer TE. Maternal nutrition and fetal development. J Nutr. 2004 Sep;134(9):2169-72. doi: 10.1093/jn/134.9.2169. PMID: 15333699.
2. Govoni KE, Reed SA, Zinn SA. CELL BIOLOGY SYMPOSIUM: METABOLIC RESPONSES TO STRESS: FROM ANIMAL TO CELL: Poor maternal nutrition during gestation: effects on offspring whole-body and tissue-specific metabolism in livestock species1,2. J Anim Sci. 2019 Jul 2;97(7):3142-3152. doi: 10.1093/jas/skz157. PMID: 31070226; PMCID: PMC6606510.
3. Desai M, Crowther NJ, Lucas A, Hales CN. Organ-selective growth in the offspring of protein-restricted mothers. Br J Nutr. 1996 Oct;76(4):591-603. doi: 10.1079/bjn19960065. PMID: 8942365.

bioRxiv preprint doi: https://doi.org/10.1101/2024.05.02.592246; this version posted May 5, 2024. The copyright holder for this preprint (which was not certified by peer review) is the author/funder, who has granted bioRxiv a license to display the preprint in perpetuity. It is made available under aCC-BY-NC-ND 4.0 International license.

4. Gruppuso PA, Boylan JM, Anand P, Bienieki TC. Effects of maternal starvation on hepatocyte proliferation in the late gestation fetal rat. Pediatr Res. 2005 Feb;57(2):185-91. doi:10.1203/01.PDR.0000151646.55587.0F. Epub 2004 Dec 20. PMID: 15611345.
5. Chadio S, Kotsampasi B, Taka S, Liandris E, Papadopoulos N, Plakokefalos E. Epigenetic changes of hepatic glucocorticoid receptor in sheep male offspring undernourished in utero. Reprod Fertil Dev. 2017 Sep;29(10):1995-2004. doi: 10.1071/RD16276. PMID: 28076749.
6. Muroya S, Zhang Y, Otomaru K, Oshima K, Oshima I, Sano M, Roh S, Ojima K, Gotoh T. Maternal Nutrient Restriction Disrupts Gene Expression and Metabolites Associated with Urea Cycle, Steroid Synthesis, Glucose Homeostasis, and Glucuronidation in Fetal Calf Liver. Metabolites. 2022 Feb 24;12(3):203. doi: 10.3390/metabo12030203. PMID: 35323646; PMCID: PMC8949217.
7. Kakadia JH, Jain BB, Biggar K, Sutherland A, Nygard K, Li C, Nathanielsz PW, Jansson T, Gupta MB. Hyperphosphorylation of fetal liver IGFBP-1 precedes slowing of fetal growth in nutrient-restricted baboons and may be a mechanism underlying IUGR. Am J Physiol Endocrinol Metab. 2020 Sep 1;319(3):E614-E628. doi: 10.1152/ajpendo.00220.2020. Epub 2020 Aug 3. PMID: 32744097; PMCID: PMC7642856.
8. Man J, Hutchinson JC, Ashworth M, Jeffrey I, Heazell AE, Sebire NJ. Organ weights and ratios for postmortem identification of fetal growth restriction: utility and confounding factors. Ultrasound Obstet Gynecol. 2016 Nov;48(5):585-590. doi: 10.1002/uog.16017. Epub 2016 Oct 25. PMID: 27781326.
9. Zhou X, Yang H, Yan Q, Ren A, Kong Z, Tang S, Han X, Tan Z, Salem AZM. Evidence for liver energy metabolism programming in offspring subjected to intrauterine undernutrition during mid gestation. Nutr Metab (Lond). 2019 Mar 18;16:20. doi: 10.1186/s12986-019-0346-7. PMID: 30923555; PMCID: PMC6423887.
10. Hellmuth C, Uhl O, Kirchberg FF, Harder U, Peissner W, Koletzko B, Nathanielsz PW. Influence of moderate maternal nutrition restriction on the fetal baboon metabolome at 0.5 and 0.9 gestation. Nutr Metab Cardiovasc Dis. 2016 Sep;26(9):786-96. doi: 10.1016/j.numecd.2016.04.004. Epub 2016 Apr 14. PMID: 27146364.
11. Li C, Schlabritz-Loutsevitch NE, Hubbard GB, Han V, Nygard K, Cox LA, McDonald TJ, Nathanielsz PW. Effects of maternal global nutrient restriction on fetal baboon hepatic insulin-like growth factor system genes and gene products. Endocrinology. 2009 Oct;150(10):4634-42. doi: 10.1210/en.2008-1648. Epub 2009 Jul 2. PMID: 19574404; PMCID: PMC2754676.
12. Hyatt MA, Gopalakrishnan GS, Bispham J, Gentili S, McMillen IC, Rhind SM, Rae MT, Kyle CE, Brooks AN, Jones C, Budge H, Walker D, Stephenson T, Symonds ME. Maternal nutrient restriction in early pregnancy programs hepatic mRNA expression of growth-related genes and liver size in adult male sheep. J Endocrinol. 2007 Jan;192(1):87-97. doi: 10.1677/joe.1.06801. PMID: 17210746.
13. George LA, Zhang L, Tuersunjiang N, Ma Y, Long NM, Uthlaut AB, Smith DT, Nathanielsz PW, Ford SP. Early maternal undernutrition programs increased feed intake, altered glucose metabolism and insulin secretion, and liver function in aged female offspring. Am J Physiol Regul Integr Comp Physiol. 2012 Apr;302(7):R795-804. doi: 10.1152/ajpregu.00241.2011. Epub 2012 Jan 25. PMID: 22277936; PMCID: PMC3330774.

bioRxiv preprint doi: https://doi.org/10.1101/2024.05.02.592246; this version posted May 5, 2024. The copyright holder for this preprint (which was not certified by peer review) is the author/funder, who has granted bioRxiv a license to display the preprint in perpetuity. It is made available under aCC-BY-NC-ND 4.0 International license.

14. Cox LA, Comuzzie AG, Havill LM, Karere GM, Spradling KD, Mahaney MC, Nathanielsz PW, Nicolella DP, Shade RE, Voruganti S, VandeBerg JL. Baboons as a model to study genetics and epigenetics of human disease. ILAR J. 2013;54(2):106-21. doi: 10.1093/ilar/ilt038. PMID: 24174436; PMCID: PMC3924757.
15. Choi J, Li C, McDonald TJ, Comuzzie A, Mattern V, Nathanielsz PW. Emergence of insulin resistance in juvenile baboon offspring of mothers exposed to moderate maternal nutrient reduction. Am J Physiol Regul Integr Comp Physiol. 2011 Sep;301(3):R757-62. doi: 10.1152/ajpregu.00051.2011. Epub 2011 Jun 8. PMID: 21653880; PMCID: PMC3174762.
16. Grijalva J, Vakili K. Neonatal liver physiology. Semin Pediatr Surg. 2013 Nov;22(4):185-9. doi: 10.1053/j.sempedsurg.2013.10.006. Epub 2013 Oct 14. PMID: 24331092.
17. Gyllenhammer LE, Entringer S, Buss C, Wadhwa PD. Developmental programming of mitochondrial biology: a conceptual framework and review. Proc Biol Sci. 2020 May 13;287(1926):20192713. doi: 10.1098/rspb.2019.2713. Epub 2020 Apr 29. PMID: 32345161; PMCID: PMC7282904.
18. Pereira SP, Tavares LC, Duarte AI, Baldeiras I, Cunha-Oliveira T, Martins JD, Santos MS, Maloyan A, Moreno AJ, Cox LA, Li C, Nathanielsz PW, Nijland MJ, Oliveira PJ. Sex-dependent vulnerability of fetal nonhuman primate cardiac mitochondria to moderate maternal nutrient reduction. Clin Sci (Lond). 2021 May 14;135(9):1103-1126. doi: 10.1042/CS20201339. PMID: 33899910; PMCID: PMC8456369.
19. Zander-Fox DL, Fullston T, McPherson NO, Sandeman L, Kang WX, Good SB, Spillane M, Lane M. Reduction of Mitochondrial Function by FCCP During Mouse Cleavage Stage Embryo Culture Reduces Birth Weight and Impairs the Metabolic Health of Offspring. Biol Reprod. 2015 May;92(5):124. doi: 10.1095/biolreprod.114.123489. Epub 2015 Feb 25. PMID: 25715796.
20. Haas RH. 2019. Mitochondrial dysfunction in aging and diseases of aging. *Biology (Basel)* **8**, 48 (10.3390/biology8020048)
21. Salmon AB, Dorigatti J, Huber HF, Li C, Nathanielsz PW. Maternal nutrient restriction in baboon programs later-life cellular growth and respiration of cultured skin fibroblasts: a potential model for the study of aging-programming interactions. Geroscience. 2018 Jun;40(3):269-278. doi: 10.1007/s11357-018-0024-0. Epub 2018 May 25. PMID: 29802507; PMCID: PMC6060193.
22. Schlabritz-Loutsevitch NE, Howell K, Rice K, Glover EJ, Nevill CH, Jenkins SL, Bill Cummins L, Frost PA, McDonald TJ, Nathanielsz PW. Development of a system for individual feeding of baboons maintained in an outdoor group social environment. J Med Primatol. 2004 Jun;33(3):117-26. doi: 10.1111/j.1600-0684.2004.00067.x. PMID: 15102068.
23. Li C, Jenkins S, Mattern V, Comuzzie AG, Cox LA, Huber HF, Nathanielsz PW. Effect of moderate, 30 percent global maternal nutrient reduction on fetal and postnatal baboon phenotype. J Med Primatol. 2017 Dec;46(6):293-303. doi: 10.1111/jmp.12290. Epub 2017 Jul 26. PMID: 28744866; PMCID: PMC5673574.
24. Li C, McDonald TJ, Wu G, Nijland MJ, Nathanielsz PW. Intrauterine growth restriction alters term fetal baboon hypothalamic appetitive peptide balance. J Endocrinol. 2013 Apr 29;217(3):275-82. doi: 10.1530/JOE-13-0012. PMID: 23482706; PMCID: PMC4018765.

bioRxiv preprint doi: https://doi.org/10.1101/2024.05.02.592246; this version posted May 5, 2024. The copyright holder for this preprint (which was not certified by peer review) is the author/funder, who has granted bioRxiv a license to display the preprint in perpetuity. It is made available under aCC-BY-NC-ND 4.0 International license.

25. Ouwerkerk R, Pettigrew RI, Gharib AM. Liver metabolite concentrations measured with 1H MR spectroscopy. Radiology. 2012 Nov;265(2):565-75. doi: 10.1148/radiol.12112344. Epub 2012 Aug 13. PMID: 22891360; PMCID: PMC3480817.
26. Naressi A, Couturier C, Devos JM, Janssen M, Mangeat C, de Beer R, Graveron-Demilly D. Java-based graphical user interface for the MRUI quantitation package. MAGMA. 2001 May;12(2-3):141-52. doi: 10.1007/BF02668096. PMID: 11390270.
27. Hamilton G, Yokoo T, Bydder M, Cruite I, Schroeder ME, Sirlin CB, Middleton MS. In vivo characterization of the liver fat ^{1}H MR spectrum. NMR Biomed. 2011 Aug;24(7):784-90. doi: 10.1002/nbm.1622. Epub 2010 Dec 12. PMID: 21834002; PMCID: PMC3860876.
28. Boesch C, Machann J, Vermathen P, Schick F. Role of proton MR for the study of muscle lipid metabolism. NMR Biomed. 2006 Nov;19(7):968-88. doi: 10.1002/nbm.1096. PMID: 17075965.
29. Muneeza A. Esani, The Physiological Sources of, Clinical Significance of, and Laboratory-Testing Methods for Determining Enzyme Levels, *Laboratory Medicine*, Volume 45, Issue 1, February 2014, Pages e16–e18,
30. Seglen PO. Preparation of isolated rat liver cells. Methods Cell Biol. 1976;13:29-83. doi: 10.1016/s0091-679x(08)61797-5. PMID: 177845.
31. Lee SM, Schelcher C, Demmel M, Hauner M, Thasler WE. Isolation of human hepatocytes by a two-step collagenase perfusion procedure. J Vis Exp. 2013 Sep 3;(79):50615. doi: 10.3791/50615. PMID: 24056912; PMCID: PMC3857361
32. Adekunbi DA, Huber HF, Li C, Nathanielsz PW, Cox LA, Salmon AB. Differential mitochondrial bioenergetics and cellular resilience in astrocytes, hepatocytes, and fibroblasts from aging baboons. Geroscience. 2024 Apr 12. doi: 10.1007/s11357-024-01155-7. Epub ahead of print. PMID: 38607532.
33. Smith PK, Krohn RI, Hermanson GT, Mallia AK, Gartner FH, Provenzano MD, Fujimoto EK, Goeke NM, Olson BJ, Klenk DC. Measurement of protein using bicinchoninic acid. Anal Biochem. 1985 Oct;150(1):76-85. doi: 10.1016/0003-2697(85)90442-7. Erratum in: Anal Biochem 1987 May 15;163(1):279. PMID: 3843705.
34. Guo C, Li C, Myatt L, Nathanielsz PW, Sun K. Sexually dimorphic effects of maternal nutrient reduction on expression of genes regulating cortisol metabolism in fetal baboon adipose and liver tissues. Diabetes. 2013 Apr;62(4):1175-85. doi: 10.2337/db12-0561. Epub 2012 Dec 13. PMID: 23238295; PMCID: PMC3609578.
35. Kuo AH, Li C, Mattern V, Huber HF, Comuzzie A, Cox L, Schwab M, Nathanielsz PW, Clarke GD. Sex-dimorphic acceleration of pericardial, subcutaneous, and plasma lipid increase in offspring of poorly nourished baboons. Int J Obes (Lond). 2018 Jun;42(5):1092-1096. doi: 10.1038/s41366-018-0008-2. Epub 2018 Jan 30. PMID: 29463919; PMCID: PMC6019612.
36. Martin LJ, Mahaney MC, Bronikowski AM, Carey KD, Dyke B, Comuzzie AG. Lifespan in captive baboons is heritable. Mech Ageing Dev. 2002 Sep;123(11):1461-7. doi: 10.1016/s0047-6374(02)00083-0. PMID: 12425953.

bioRxiv preprint doi: https://doi.org/10.1101/2024.05.02.592246; this version posted May 5, 2024. The copyright holder for this preprint (which was not certified by peer review) is the author/funder, who has granted bioRxiv a license to display the preprint in perpetuity. It is made available under aCC-BY-NC-ND 4.0 International license.

37. Bronikowski AM, Alberts SC, Altmann J, Packer C, Carey KD, Tatar M. The aging baboon: comparative demography in a non-human primate. Proc Natl Acad Sci U S A. 2002 Jul 9;99(14):9591-5. doi: 10.1073/pnas.142675599. Epub 2002 Jun 24. PMID: 12082185; PMCID: PMC123185.
38. Von Schulze A, McCoin CS, Onyekere C, Allen J, Geiger P, Dorn GW 2nd, Morris EM, Thyfault JP. Hepatic mitochondrial adaptations to physical activity: impact of sexual dimorphism, PGC1α and BNIP3-mediated mitophagy. J Physiol. 2018 Dec;596(24):6157-6171. doi: 10.1113/JP276539. Epub 2018 Aug 28. PMID: 30062822; PMCID: PMC6292817.
39. Hart-Unger S, Arao Y, Hamilton KJ, Lierz SL, Malarkey DE, Hewitt SC, Freemark M, Korach KS. Hormone signaling and fatty liver in females: analysis of estrogen receptor α mutant mice. Int J Obes (Lond). 2017 Jun;41(6):945-954. doi: 10.1038/ijo.2017.50. Epub 2017 Feb 21. PMID: 28220039; PMCID: PMC5735425.
40. Parlee SD, MacDougald OA. Maternal nutrition and risk of obesity in offspring: the Trojan horse of developmental plasticity. Biochim Biophys Acta. 2014 Mar;1842(3):495-506. doi: 10.1016/j.bbadis.2013.07.007. Epub 2013 Jul 16. PMID: 23871838; PMCID: PMC3855628.
41. VandeBerg JL, Williams-Blangero S. Advantages and limitations of nonhuman primates as animal models in genetic research on complex diseases. J Med Primatol. 1997 Jun;26(3):113-9. doi: 10.1111/j.1600-0684.1997.tb00042.x. PMID: 9379477.
42. Chen JP, Peng B, Tang L, Sun R, Hu S, Wen XY, Que P, Wang YH. Fetal and infant exposure to the Chinese famine increases the risk of fatty liver disease in Chongqing, China. J Gastroenterol Hepatol. 2016 Jan;31(1):200-5. doi: 10.1111/jgh.13044. PMID: 26201820.
43. Sandboge S, Perälä MM, Salonen MK, Blomstedt PA, Osmond C, Kajantie E, Barker DJ, Eriksson JG. Early growth and non-alcoholic fatty liver disease in adulthood-the NAFLD liver fat score and equation applied on the Helsinki Birth Cohort Study. Ann Med. 2013 Sep;45(5-6):430-7. doi: 10.3109/07853890.2013.801275. Epub 2013 Jun 14. PMID: 23767967.
44. George LA, Zhang L, Tuersunjiang N, Ma Y, Long NM, Uthlaut AB, Smith DT, Nathanielsz PW, Ford SP. Early maternal undernutrition programs increased feed intake, altered glucose metabolism and insulin secretion, and liver function in aged female offspring. Am J Physiol Regul Integr Comp Physiol. 2012 Apr;302(7):R795-804. doi: 10.1152/ajpregu.00241.2011. Epub 2012 Jan 25. PMID: 22277936; PMCID: PMC3330774.
45. Hoffman JM, Valencak TG. A short life on the farm: aging and longevity in agricultural, large-bodied mammals. Geroscience. 2020 Jun;42(3):909-922. doi: 10.1007/s11357-020-00190-4. Epub 2020 May 2. PMID: 32361879; PMCID: PMC7286991.
46. Rector RS, Thyfault JP, Uptergrove GM, Morris EM, Naples SP, Borengasser SJ, Mikus CR, Laye MJ, Laughlin MH, Booth FW, Ibdah JA. Mitochondrial dysfunction precedes insulin resistance and hepatic steatosis and contributes to the natural history of non-alcoholic fatty liver disease in an obese rodent model. J Hepatol. 2010 May;52(5):727-36. doi: 10.1016/j.jhep.2009.11.030. Epub 2010 Mar 4. PMID: 20347174; PMCID: PMC3070177.
47. McConnell JM, Petrie L. Mitochondrial DNA turnover occurs during preimplantation development and can be modulated by environmental factors. Reprod Biomed Online. 2004 Oct;9(4):418-24. doi: 10.1016/s1472-6483(10)61277-1. PMID: 15511342.

bioRxiv preprint doi: https://doi.org/10.1101/2024.05.02.592246; this version posted May 5, 2024. The copyright holder for this preprint (which was not certified by peer review) is the author/funder, who has granted bioRxiv a license to display the preprint in perpetuity. It is made available under aCC-BY-NC-ND 4.0 International license.

48. Andreas E, Reid M, Zhang W, Moley KH. The effect of maternal high-fat/high-sugar diet on offspring oocytes and early embryo development. Mol Hum Reprod. 2019 Nov 30;25(11):717-728. doi: 10.1093/molehr/gaz049. PMID: 31588490; PMCID: PMC6884416.
49. de Velasco PC, Chicaybam G, Ramos-Filho DM, Dos Santos RMAR, Mairink C, Sardinha FLC, El-Bacha T, Galina A, Tavares-do-Carmo MDG. Maternal intake of trans-unsaturated or interesterified fatty acids during pregnancy and lactation modifies mitochondrial bioenergetics in the liver of adult offspring in mice. Br J Nutr. 2017 Jul;118(1):41-52. doi: 10.1017/S0007114517001817. Epub 2017 Aug 11. PMID: 28797310.
50. Li C, Ramahi E, Nijland MJ, Choi J, Myers DA, Nathanielsz PW, McDonald TJ. Up-regulation of the fetal baboon hypothalamo-pituitary-adrenal axis in intrauterine growth restriction: coincidence with hypothalamic glucocorticoid receptor insensitivity and leptin receptor down-regulation. Endocrinology. 2013 Jul;154(7):2365-73. doi: 10.1210/en.2012-2111. Epub 2013 Apr 26. PMID: 23625543; PMCID: PMC3689287.
51. Du J, McEwen B, Manji HK. Glucocorticoid receptors modulate mitochondrial function: A novel mechanism for neuroprotection. Commun Integr Biol. 2009 Jul;2(4):350-2. doi: 10.4161/cib.2.4.8554. PMID: 19721888; PMCID: PMC2734045.
52. Hou C, Amunugama K. On the complex relationship between energy expenditure and longevity: Reconciling the contradictory empirical results with a simple theoretical model. Mech Ageing Dev. 2015 Jul;149:50-64. doi: 10.1016/j.mad.2015.06.003. Epub 2015 Jun 15. PMID: 26086438.
53. Bobba-Alves N, Juster RP, Picard M. The energetic cost of allostasis and allostatic load. Psychoneuroendocrinology. 2022 Dec;146:105951. doi: 10.1016/j.psyneuen.2022.105951. Epub 2022 Oct 8. PMID: 36302295; PMCID: PMC10082134.
54. Hüttemann M, Pecina P, Rainbolt M, Sanderson TH, Kagan VE, Samavati L, Doan JW, Lee I. The multiple functions of cytochrome c and their regulation in life and death decisions of the mammalian cell: From respiration to apoptosis. Mitochondrion. 2011 May;11(3):369-81. doi: 10.1016/j.mito.2011.01.010. Epub 2011 Feb 4. PMID: 21296189; PMCID: PMC3075374.
55. Bobba-Alves N, Sturm G, Lin J, Ware SA, Karan KR, Monzel AS, Bris C, Procaccio V, Lenaers G, Higgins-Chen A, Levine M, Horvath S, Santhanam BS, Kaufman BA, Hirano M, Epel E, Picard M. Cellular allostatic load is linked to increased energy expenditure and accelerated biological aging. Psychoneuroendocrinology. 2023 Sep;155:106322. doi: 10.1016/j.psyneuen.2023.106322. Epub 2023 Jun 14. PMID: 37423094; PMCID: PMC10528419.
56. Gyllenhammer LE, Picard M, McGill MA, Boyle KE, Vawter MP, Rasmussen JM, Buss C, Entringer S, Wadhwa PD. Prospective association between maternal allostatic load during pregnancy and child mitochondrial content and bioenergetic capacity. Psychoneuroendocrinology. 2022 Oct;144:105868. doi: 10.1016/j.psyneuen.2022.105868. Epub 2022 Jul 15. PMID: 35853381; PMCID: PMC9706402.
57. Williams ED, Rogers SC, Zhang X, Azhar G, Wei JY. Elevated oxygen consumption rate in response to acute low-glucose stress: Metformin restores rate to normal level. Exp Gerontol. 2015 Oct;70:157-62. doi: 10.1016/j.exger.2015.08.002. Epub 2015 Aug 7. PMID: 26256471; PMCID: PMC4654776.
58. Weightman Potter PG, Vlachaki Walker JM, Robb JL, Chilton JK, Williamson R, Randall AD, Ellacott KLJ, Beall C. Basal fatty acid oxidation increases after recurrent low glucose in human primary astrocytes.

bioRxiv preprint doi: https://doi.org/10.1101/2024.05.02.592246; this version posted May 5, 2024. The copyright holder for this preprint (which was not certified by peer review) is the author/funder, who has granted bioRxiv a license to display the preprint in perpetuity. It is made available under aCC-BY-NC-ND 4.0 International license.

Diabetologia. 2019 Jan;62(1):187-198. doi: 10.1007/s00125-018-4744-6. Epub 2018 Oct 6. PMID: 30293112; PMCID: PMC6290858.

59. Elkalaf M, Anděl M, Trnka J. Low glucose but not galactose enhances oxidative mitochondrial metabolism in C2C12 myoblasts and myotubes. PLoS One. 2013 Aug 5;8(8):e70772. doi: 10.1371/journal.pone.0070772. PMID: 23940640; PMCID: PMC3733643.

bioRxiv preprint doi: https://doi.org/10.1101/2024.05.02.592246; this version posted May 5, 2024. The copyright holder for this preprint (which was not certified by peer review) is the author/funder, who has granted bioRxiv a license to display the preprint in perpetuity. It is made available under aCC-BY-NC-ND 4.0 International license.

643 **Figure Legends**

644 **Fig. 1**: Liver metabolites in control and MUN baboon offspring. Liver metabolites were determined by magnetic
645 resonance spectroscopy in female and male subjects from control and MUN groups (a) Liver glycogen
646 concentration. (b) Liver choline concentration. (c) Liver lipid concentration. (d) Liver glycogen concentration for
647 combined sexes (b) Liver choline concentration for combined sexes. (c) Liver lipid concentration for combined
648 sexes. Black bars represent control baboons while clear bars are MUN baboons. Each dot represents an individual
649 animal. Data are expressed as mean ± SEM, sample size and age range (control; n=10 for females, 12.4-
650 16.4 years, 6 for males, 12.1-17.2, MUN; n=7 for females, 12.3-14.7 years, 6 for males, 12.4-15.0 years). For
651 interaction of sex and treatment, data were analyzed by two-way ANOVA, while student's t-test was used for
652 treatment group comparison using GraphPad prism 9. Abbreviations: CTR; Control, MUN; maternal undernutrition.

653 Fig. 2: Plasma enzyme levels in control and MUN baboon offspring. (a) Aspartate aminotransferase levels in female
654 and male subjects in the control and MUN groups. (b) Alkaline phosphatase levels in control and MUN baboons of
655 both sexes. (c) Alanine transaminase levels in female and male baboons from control and MUN groups. (d)
656 Aspartate aminotransferase levels for combined sexes in control and MUN groups. (e) Alkaline phosphatase levels
657 for combined sexes in control and MUN groups. (f) Alanine transaminase levels for combined sexes in control and
658 MUN groups. Black bars are for control baboons while clear bars are MUN baboons. Each dot represents an
659 individual animal. Data are expressed as mean ± SEM, sample size (control; n=10 for females, 6 for males, MUN;
660 n=7 for females, 6 for males). Age range: Control female and male baboons; 13.3-17.8 and 13.6-18.0 respectively,
661 MUN females; 13.1-16.0 years, MUN males; 13.4–16.0 years. Two-way ANOVA was used determine sex and
662 treatment interactions. When sexes were combined, difference between control and MUN baboons were
663 determined by student's t-test using GraphPad prism 9.

664 Fig. 3: Viability of hepatocytes derived from control and MUN baboon offspring. (a) Number of live hepatocytes per
665 gram of liver tissue (b) Hepatocyte viability. Data from left and right liver lobes were combined given that there were
666 no lobe-specific differences. Each dot represents data point from individual liver lobes of each animal. Sample size;
667 control females, n=6, control males, n=6, MUN females, n=6, MUN males, n=5.

668 Fig. 4: Cellular respiration in control and MUN baboon offspring. Oxygen consumption rate (OCR) and extracellular
669 acidification rate in hepatocytes derived from MUN baboons and their control counterparts. OCR response to
670 mitochondrial modulators such as oligomycin, FCCP and rotenone/antimycin were used to ATP-linked, and
671 maximal respiration. Tetramethylrhodamine ethyl ester (TMRE) based assay was used to determine mitochondrial
672 membrane potential (a) Basal respiration. (b) ATP-linked respiration. (c) Maximal respiration. (d) Spare respiratory
673 capacity. (e) Basal ECAR. (f) Basal OCR to ECAR ratio. (g) Mitochondrial membrane potential. Data were
674 expressed as mean ± SEM, with left and right liver hepatocyte data combined. OCR and ECAR were from 4 to 6
675 replicate samples and were measured using a seahorse XFe96 flux analyzer. OCR and ECAR data were
676 normalized to cell density determined by a live-cell imager (IncuCyte). Seahorse assay sample size; control
677 females, n=6, control males, n=5, MUN females, n=6, MUN males, n=4. TMRE assay sample size: control females,
678 n=6, control males, n=3, MUN females, n=4, MUN males, n=4.

679 Fig. 5: Cellular respiration in response to metabolic stress in control and MUN baboon offspring. Hepatocytes
680 derived from male and female baboons in control and MUN groups were exposed to low glucose media (1 mM) for

bioRxiv preprint doi: https://doi.org/10.1101/2024.05.02.592246; this version posted May 5, 2024. The copyright holder for this preprint (which was not certified by peer review) is the author/funder, who has granted bioRxiv a license to display the preprint in perpetuity. It is made available under aCC-BY-NC-ND 4.0 International license.

2 h to model metabolic stress prior to mitochondrial stress test. Standard hepatocyte culture media contains 11.1 mM glucose. (a) Female basal respiration. (b) Female ATP-linked respiration. (c) Female maximal respiration. (d) Female spare respiratory capacity. (e) Male basal respiration. (f) Male ATP-linked respiration. (g) Male maximal respiration. (h) Male spare respiratory capacity. Data were expressed as mean ± SEM, with left and right liver hepatocyte data combined. OCR were from 4 to 6 replicate samples and were measured using a seahorse XFe96 flux analyzer. OCR and ECAR data were normalized to cell density. Sample size; control females, n=6, control males, n=5, MUN females, n=6, MUN males, n=4.

Fig. 6: Mitochondrial electron transport chain subunits protein abundance in hepatocytes of control and MUN baboon offspring. Bar graphs present average normalized level of indicated mitochondrial subunit protein expression ± standard error of mean (SEM). Black bars represent control baboons while clear bars are MUN baboons. (a) Complex I (NDFUB8) protein expression (b) Complex II (SDHB) expression (c) Complex III (UQCRC2) protein expression (d) Complex IV,MTCO1 protein expression. (e) Complex V (ATP5a) protein expression (f) Representative photomicrograph of protein expressions in hepatocytes of control and MUN animals. Immunoblotting data are from left liver lobe hepatocyte. Sample size; control females, n=6, control males, n=5, MUN females, n=6, MUN males, n=5.

Fig. 7: Levels of mitochondrial and antioxidant proteins in hepatocytes of control and MUN baboon offspring. Bar graphs present average normalized level of indicated mitochondrial subunit protein expression ± standard error of mean (SEM) determined by immunoblotting. (a) MFN I (b) OPA1 (c) Photomicrograph of MFN1 protein bands (d) Photomicrograph of OPA1 protein bands (e) Drp1 (f) PGC1a (g) Photomicrograph of Drp1 protein bands (h) Photomicrograph of PGC1a protein bands (i) Catalase (j) SOD2 (g) Photomicrograph of catalase and SOD2 protein bands. Immunoblotting data are from left liver lobe hepatocyte. Sample size; control females, n=6, control males, n=5, MUN females, n=6, MUN males, n=5.

Fig 1

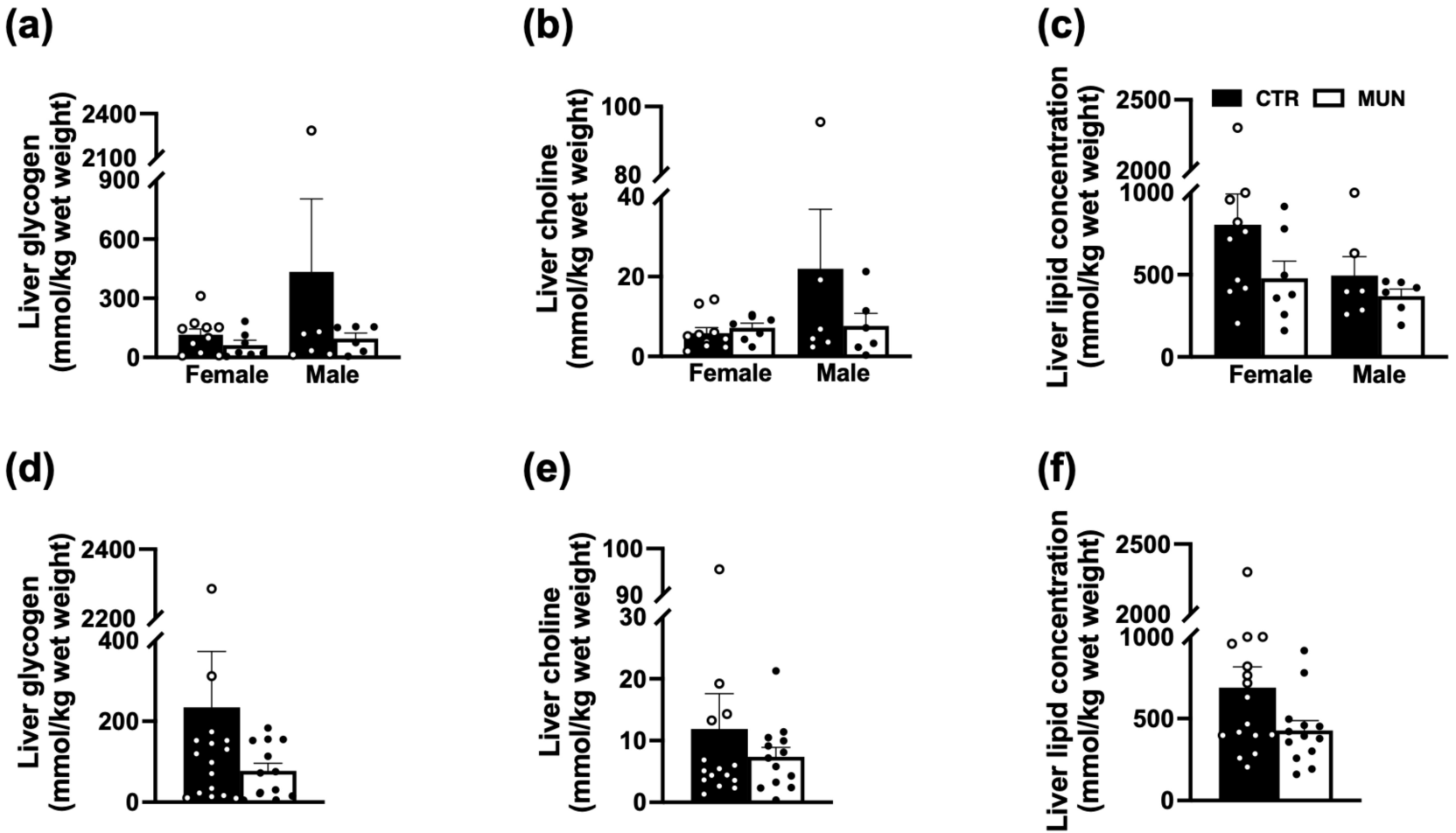
(a)
Liver glycogen (mmol/kg wet weight)
2400
2100
900
600
300
0
Female
Male
(b)
Liver choline (mmol/kg wet weight)
100
80
40
20
0
Female
Male
(c)
Liver lipid concentration (mmol/kg wet weight)
CTR
MUN
2500
2000
1000
500
0
Female
Male
(d)
Liver glycogen (mmol/kg wet weight)
2400
2200
400
200
0
(e)
Liver choline (mmol/kg wet weight)
100
90
30
20
10
0
(f)
Liver lipid concentration (mmol/kg wet weight)
2500
2000
1000
500
0

Fig 2

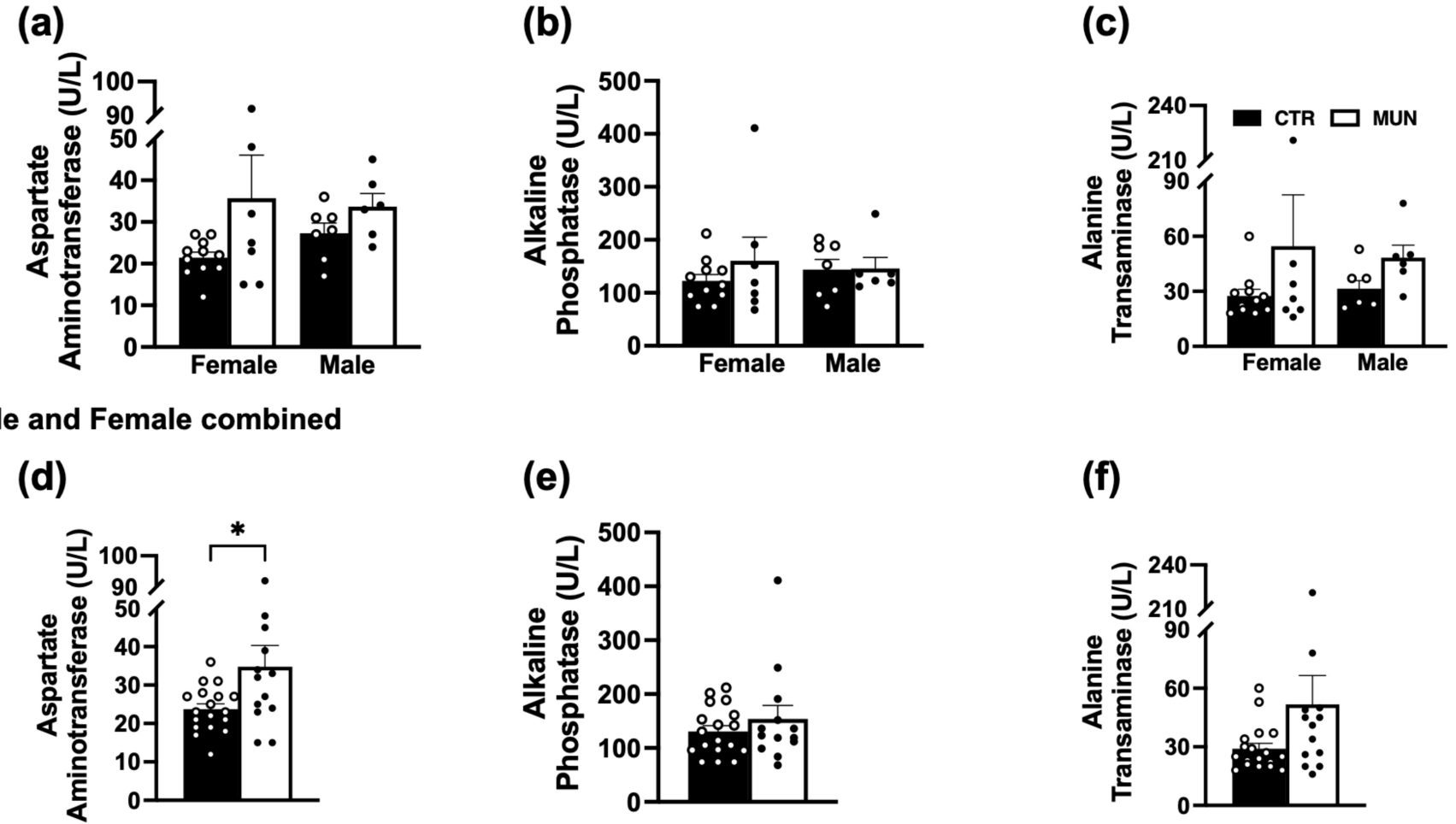
(a)
Aspartate Aminotransferase (U/L)
100
90
50
40
30
20
10
0
Female
Male
(b)
Alkaline Phosphatase (U/L)
500
400
300
200
100
0
Female
Male
(c)
Alanine Transaminase (U/L)
240
210
90
60
30
0
CTR
MUN
Female
Male
Male and Female combined
(d)
Aspartate Aminotransferase (U/L)
*
100
90
50
40
30
20
10
0
(e)
Alkaline Phosphatase (U/L)
500
400
300
200
100
0
(f)
Alanine Transaminase (U/L)
240
210
90
60
30
0

Fig 3

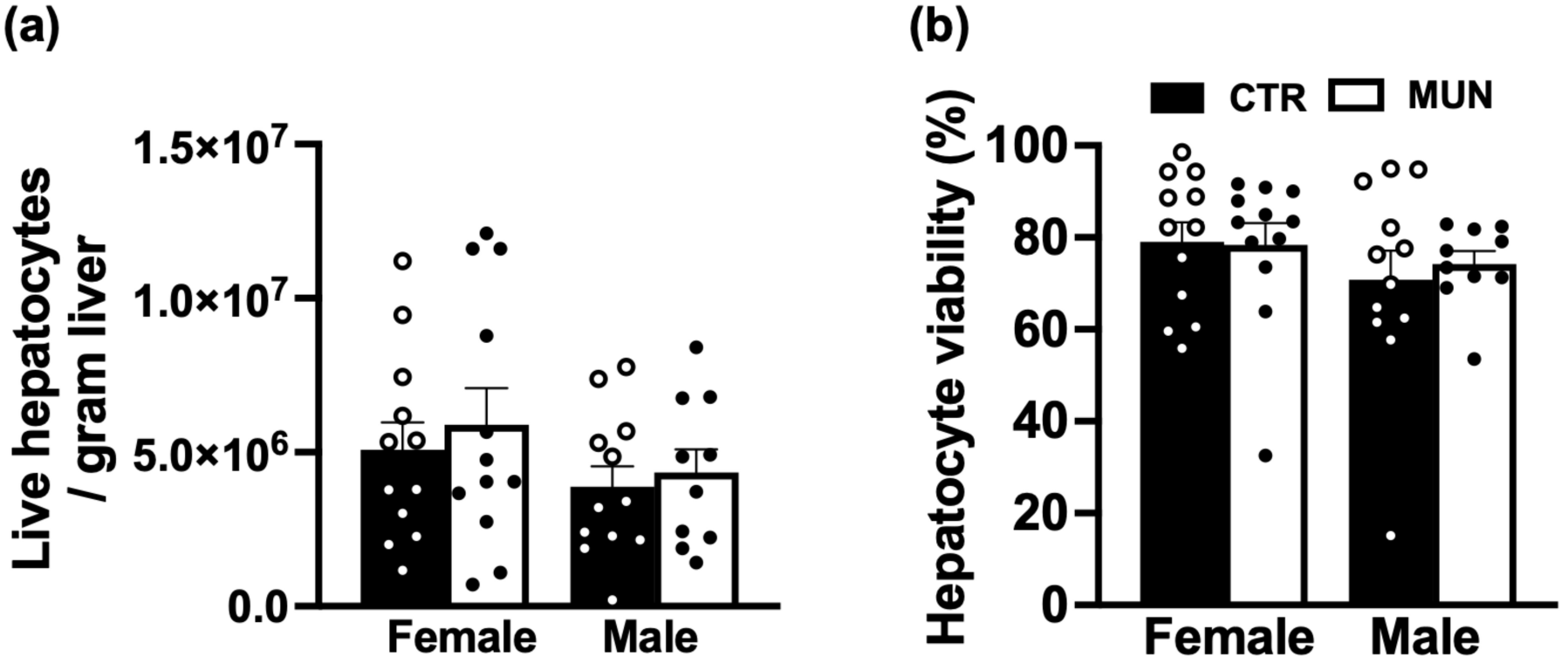
(a)
Live hepatocytes / gram liver
1.5×10^7
1.0×10^7
5.0×10^6
0.0
Female
Male
(b)
CTR
MUN
Hepatocyte viability (%)
100
80
60
40
20
0
Female
Male

Fig 4

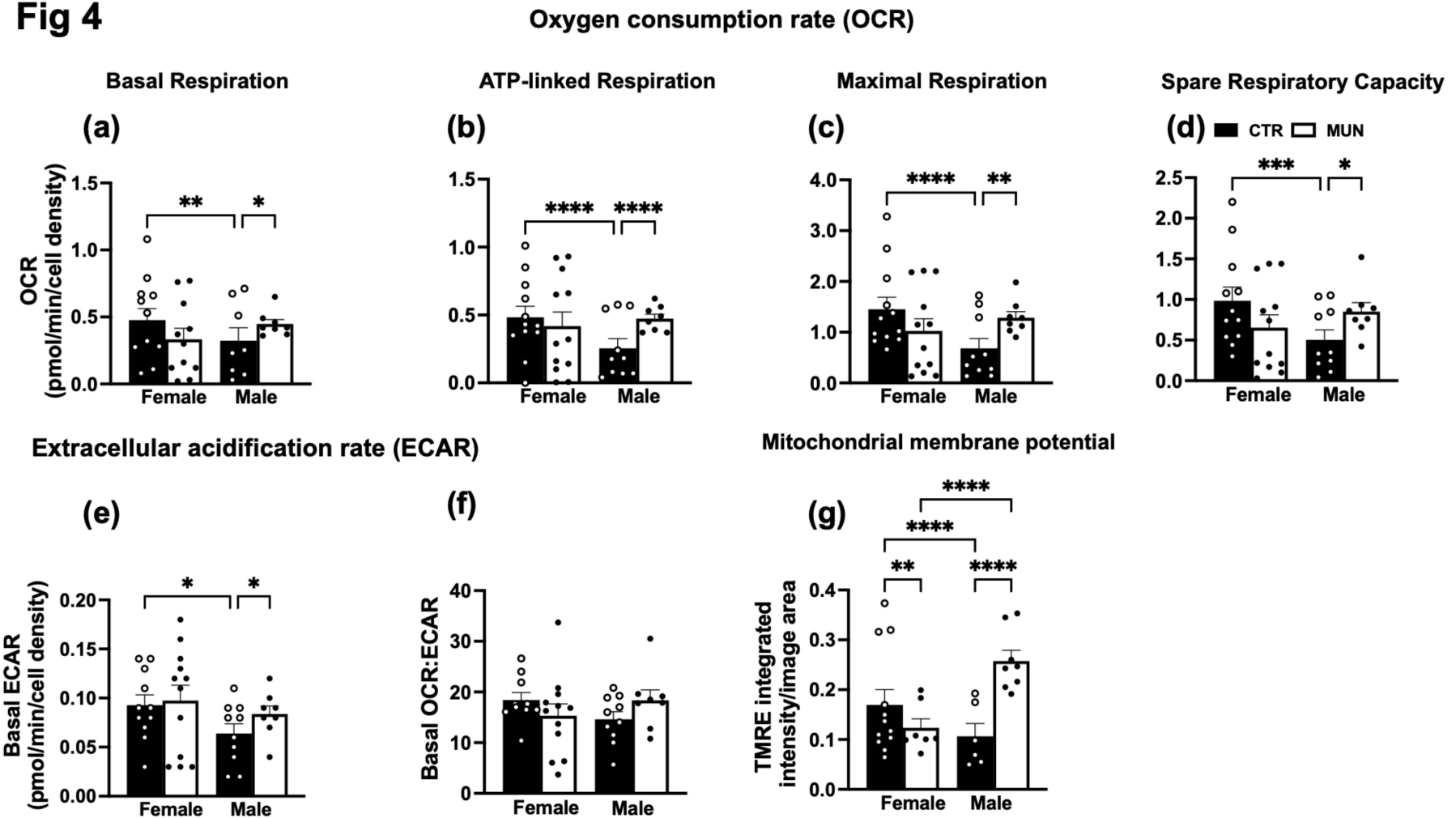
Oxygen consumption rate (OCR)
Basal Respiration
ATP-linked Respiration
Maximal Respiration
Spare Respiratory Capacity
(a)
(b)
(c)
(d)
CTR
MUN
OCR (pmol/min/cell density)
Female
Male
Extracellular acidification rate (ECAR)
Mitochondrial membrane potential
(e)
(f)
(g)
Basal ECAR (pmol/min/cell density)
Basal OCR:ECAR
TMRE integrated intensity/image area

Fig 5

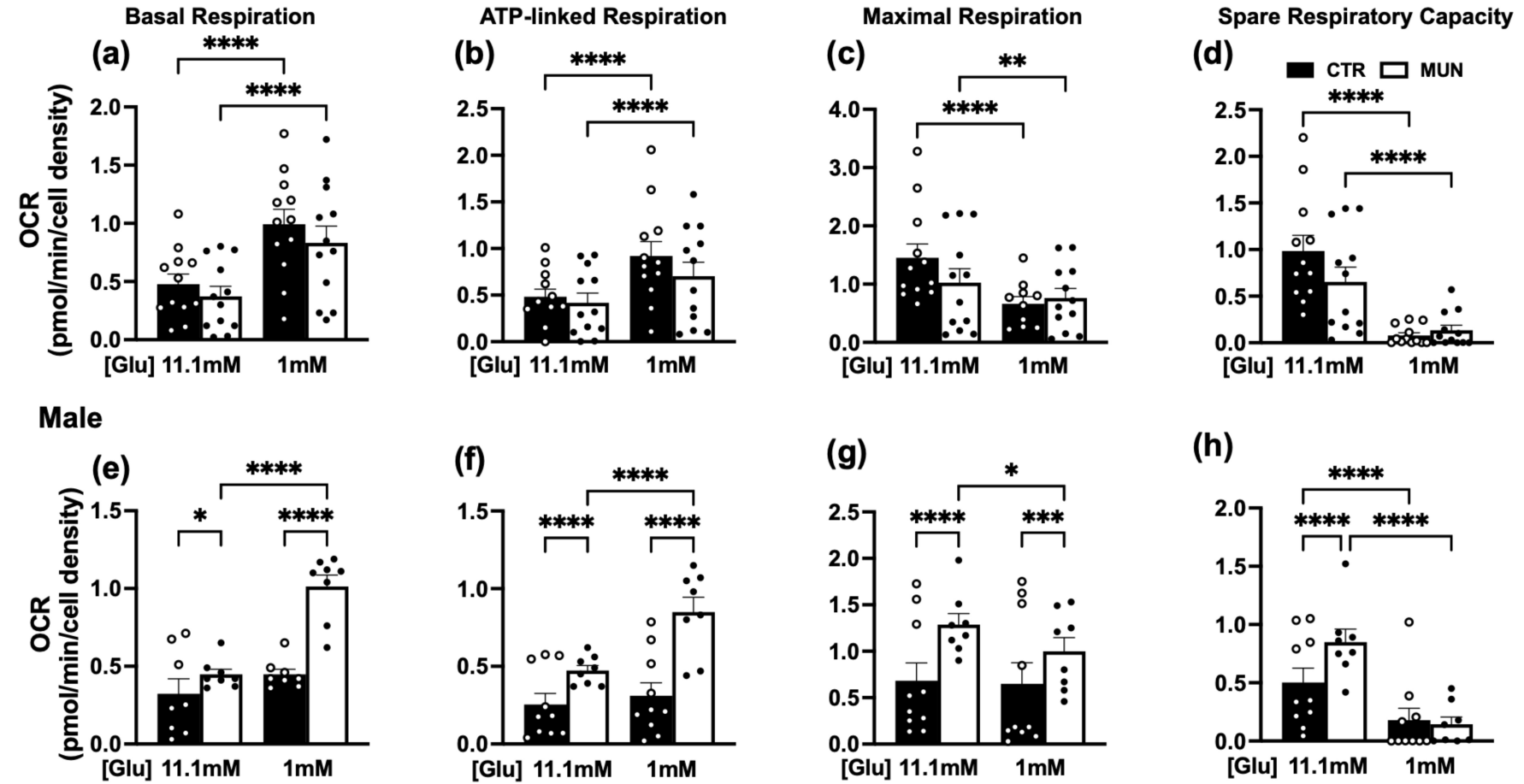
Female
Basal Respiration
ATP-linked Respiration
Maximal Respiration
Spare Respiratory Capacity
(a)
(b)
(c)
(d)
CTR
MUN
OCR (pmol/min/cell density)
[Glu] 11.1mM
1mM
Male
(e)
(f)
(g)
(h)

Fig 6

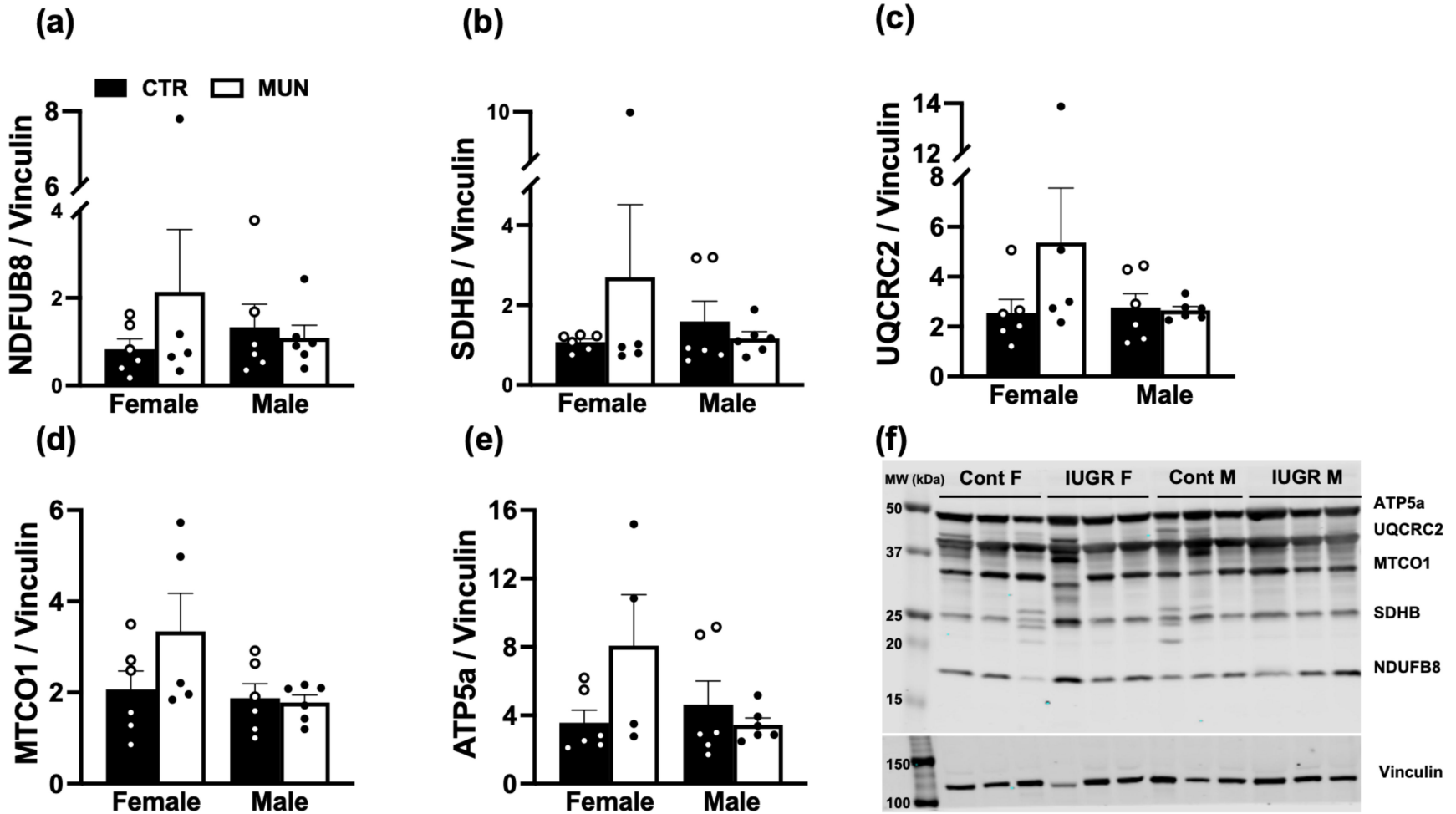
(a)
CTR
MUN
NDFUB8 / Vinculin
8
6
4
2
0
Female
Male
(b)
SDHB / Vinculin
10
4
2
0
Female
Male
(c)
UQCRC2 / Vinculin
14
12
8
6
4
2
0
Female
Male
(d)
MTCO1 / Vinculin
6
4
2
0
Female
Male
(e)
ATP5a / Vinculin
16
12
8
4
0
Female
Male
(f)
MW (kDa)
Cont F
IUGR F
Cont M
IUGR M
50
37
25
20
15
150
100
ATP5a
UQCRC2
MTCO1
SDHB
NDUFB8
Vinculin

Fig 7

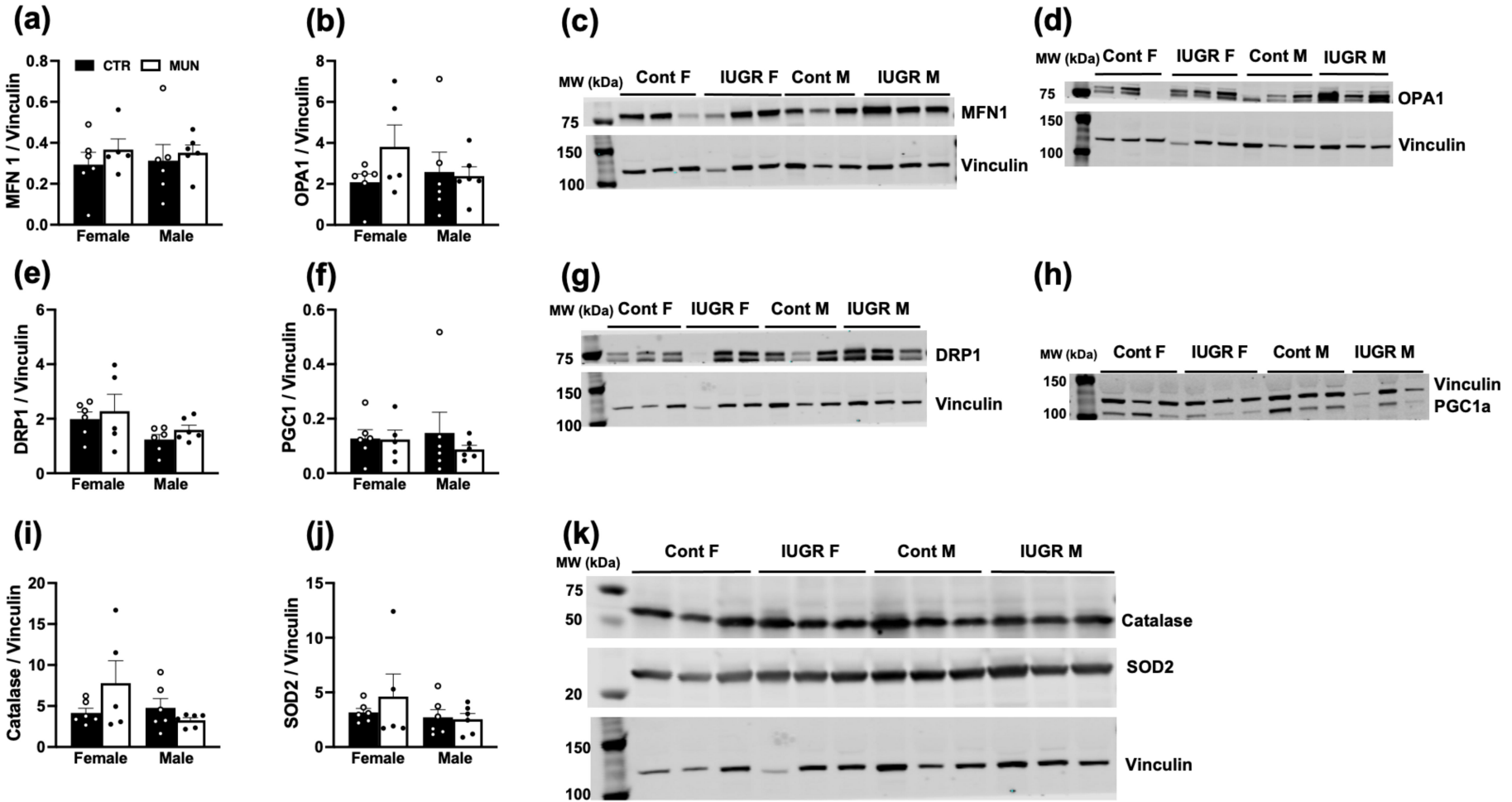
(a)
CTR
MUN
MFN 1 / Vinculin
0.8
0.6
0.4
0.2
0.0
Female
Male
(b)
OPA1 / Vinculin
8
6
4
2
0
Female
Male
(c)
MW (kDa)
Cont F
IUGR F
Cont M
IUGR M
75
150
100
MFN1
Vinculin
(d)
MW (kDa)
Cont F
IUGR F
Cont M
IUGR M
75
150
100
OPA1
Vinculin
(e)
DRP1 / Vinculin
6
4
2
0
Female
Male
(f)
PGC1 / Vinculin
0.6
0.4
0.2
0.0
Female
Male
(g)
MW (kDa)
Cont F
IUGR F
Cont M
IUGR M
75
150
100
DRP1
Vinculin
(h)
MW (kDa)
Cont F
IUGR F
Cont M
IUGR M
150
100
Vinculin
PGC1a
(i)
Catalase / Vinculin
20
15
10
5
0
Female
Male
(j)
SOD2 / Vinculin
15
10
5
0
Female
Male
(k)
MW (kDa)
Cont F
IUGR F
Cont M
IUGR M
75
50
20
150
100
Catalase
SOD2
Vinculin